ORIGINAL RESEARCH

Effect of water on the dissolution of flax fiber bundles in the ionic liquid 1-ethyl-3-methylimidazolium acetate

**Fatimah A. Albarakati · Peter J. Hine ·
Michael E. Ries**

Abstract This work investigated the dissolution rate of flax fibers in the ionic liquid 1-ethyl-3-methylimidazolium acetate [C2mim] [OAc] with the addition of a cellulose anti-solvent, water. The dissolution process was studied as a function of time, temperature and water concentration. Optical microscopy is used to analyse the resultant partially dissolved fibers. Distilled water was added to the solvent bath at the concentrations of 1%, 2% and 4% by weight in order to understand its influence on the dissolution process. The effect of the addition of even small amounts of water was found to significantly decrease the speed of dissolution, decreasing exponentially as a function of water concentration. The resulting data of both pure (as received from the manufacturers) ionic liquid and ionic liquid/anti-solvent mixtures showed the growth of the coagulated fraction as a function of both dissolution time and temperature followed time temperature superposition. An Arrhenius behavior was found, enabling the measurement of the activation energy for the dissolution of flax fiber. The activation energy of the IL as received (0.2% water) was found to be 64 ± 5 kJ/mol. For 1%, 2% and 4% water systems, the activation energies were found to be 74 ± 7 kJ/mol, 97 ± 3 kJ/mol and 116 ± 0.6 kJ/mol respectively. Extrapolating these results to zero water concentration gave a value for the hypothetical dry IL (0% water) of 58 ± 4 kJ/mol. The hypothetical dry ionic liquid is predicted to dissolve cellulose 23% faster than the IL as received (0.2% water).

Keywords Cellulose · Dissolution · Time-temperature superposition · Activation energy · Water · Ionic liquid

F. A. Albarakati
Department of Basic Science, University College in Adam, Umm Al-Qura University, Makkah, Saudi Arabia

F. A. Albarakati (✉) · P. J. Hine (✉) · M. E. Ries (✉)
School of Physics and Astronomy, University of Leeds, Woodhouse Lane, Leeds LS2 9JT, UK
e-mail: pyfma@leeds.ac.uk

P. J. Hine
e-mail: p.j.hine@leeds.ac.uk

M. E. Ries
e-mail: m.e.ries@leeds.ac.uk

Introduction

Biopolymer carbohydrates currently attract much attention as renewable materials of biomass based on products and applications, such as food packaging, materials and renewable energy (Baranwal et al. 2022; Yang et al. 2014). The biopolymer cellulose is considered to be the most abundant polymer on earth (Khademian et al. 2020). It provides researchers with a fascinating alternative to fossil fuel derivatives. Lignocellulosic biomass is estimated at an annual

production of around 10^{11} tons per year (Li et al. 2018).

Cellulose is insoluble in water and many organic solvents due to strong hydrogen bond networks in their highly ordered crystals, crystalline nature, and interactions between rings with hydrophobic tendencies (Li et al. 2020; Liang et al. 2021). Dissolving cellulose is a key step of cellulose processing, before its conversion to value-added products by coagulation with anti-solvents (Ju et al. 2022; Li et al. 2018). The coagulation process in cellulose-IL solutions involves reforming the cellulose molecules into amorphous and crystalline cellulose II (Mazlan et al. 2019). Anti-solvents are critical in reconstructing dissolved cellulose into valuable products; anti-solvents such as water, acetone, and ethanol performed effectively in regenerating dissolved cellulose, making them subjects to numerous scientific studies (Tan et al. 2019). For example, Zeng et al. compared water and ethanol anti-solvent properties, noting that water performed better when breaking cellulose-IL bonds (Zeng et al. 2020). Taokaew and Kriangkrai (2022) reported that the regeneration of cellulose with water has exhibited better thermal stability than the regeneration with ethanol (Taokaew and Kriangkrai 2022). Afterwards, the anti-solvents can be removed from the cellulose-IL solutions by a drying process to evaporate the coagulants (Huber et al. 2012). Cellulose regeneration can yield mechanically high-quality products for hydrogels, films, fibers, membranes, and many other applications.

Researchers have studied the application of numerous cellulose solvent systems, including NaOH/CS$_2$, NaOH/urea, N-methyl morpholine-N-oxide (NMMO), and many others, with commercial success in various NMMO systems (Li et al. 2020; Rosenau et al. 1999). The traditional cellulose dissolution systems have challenges that include adverse pollution, high energy and reagent consumption, solvent evaporation, and non-trivial operation processes (Yang et al. 2019). Therefore, there is still an increasing demand for developing green alternative cellulose solvents, to overcome these challenges.

Ionic liquids (ILs) are organic salts made up of cations and anions and were first synthesised by Paul Walden, who discovered the IL of ethyl ammonium nitrate ([EtNH_3] [NO_3]) with a melting point below 100°C (Walden 1914). ILs have excellent properties compared with traditional solvents, such as low vapor pressure, high thermal stability and potential recyclability (Ghandi 2014; Liu et al. 2015a, b). Therefore, over the last decades they have been shown to have great potential to be green cellulose solvents (Earle et al. 2006; Miao and Hamad 2013; Walden 1914; Yang et al. 2020). Since 1934, molten salts have been identified as playing an important role in the dissolution process of cellulose. For example, Graenacher, who dissolved cellulose in the salt (N-alkyl pyridinium chloride) at melting point 118 °C, and so not strictly an IL according to the prior Walden's definition of having a melting point below 100 °C (Plechkova and Seddon 2008). In 2002, Swatloski et al. first described the dissolution of cellulose using methyl-imidazolium - based ionic liquids with melting points below 100 °C (Swatloski et al. 2002). Since then, the dissolution of cellulose in ionic liquids has interested a number of researchers to produce and study cellulose in solution (Huber et al. 2012; Khan et al. 2018). However, It is worth noting that the purity of the IL (98% in our case) may have also impact the dissolution due to derivatizing reactions or additional side reactions (Liebner et al. 2010). Within their work, they cautioned that if the IL contains significant impurities, additional side reactions with cellulose can occur. Furthermore, (Zweckmair et al. 2015) describe the acetylating action of ILs (1,3-dialkylimidazolium acetate) with cellulose may occur with resultant impurities. They also note that ILs that are pure do not exhibit this reaction.

The potential of cellulose dissolving was investigated for many ILs, particularly room temperature ionic liquids (RT-ILs) where higher cellulose solubility was documented. For example, Zhang et al. (2005) used 1-allyl-3-methylimidazolium chloride ([AMIM][Cl]) in order to produce solutions that contained up to 5 wt% of cellulose (Zhang et al. 2005). Fukaya et al. (2008) used 1-ethyl-3-methylimidazolium methylphosphonate ([EMIM][CH_3PO_3]) to prepare solutions containing 10 wt% of cellulose (Fukaya et al. 2008). In addition to the examples given, there are certain ILs that have a solubility of up to 22% wt. of cellulose (Fukaya et al. 2006). Brehm et al. (2019) have reported that the solubility of cellulose is dependent on the anion due to the strong interaction between hydrogen bonds and anions (Brehm et al. 2019). It is widely acknowledged that the breaking up of the intra- and intermolecular hydrogen bonds in

cellulose is the crucial point in the dissolution of this polymer (Bochek 2003; Lindman et al. 2017).

In current work, water was used as an anti-solvent to investigate the dissolution of cellulose in an IL/water mixture. This is a very important area to study as among ionic liquids, imidazolium based ILs are prone to water absorption (Miyamoto et al. 2014). The absorption of water can reduce the available H-bond of the anion, and as a result, decrease the capability of dissolving cellulose (Zhao et al. 2015). Several studies have found that the presence of small amounts of water may reduce the ability of dissolving ILs, as well as the cellulose dissolution due to the moisture content (Le et al. 2012; Manna and Ghosh 2019; Mazza et al. 2009). The water content can also modify the diffusion of the cation and anion. The diffusivity of the cation is faster than the anion in the pure ionic liquid, this trend is reversed by presence of water (Hall et al. 2012; Le et al. 2012).

The presence of water can also reduce the interaction between ions due to water breaking the H-bonds between the cation and the anion (Gupta et al. 2013). Liu et al. (2015a, b) found that the interactions between cation and anion in the pure ionic liquid are stronger than in the solution. For the solution, the average interactions between anion and cation are about -1309 kJ/mol. However, the average interactions in the pure IL are much higher than the solution at around -6725 kJ/mol. This indicates that the interaction between ions is stronger in the neat IL as compared to the mixture of IL and water (Liu et al. 2015a, b).

In current work, a fundamental study of the dissolution mechanism of flax fiber bundles, and the effect of water, in an ionic liquid is reported, along with a method to measure the dissolution energy (Chen et al. 2020a) employed by our research group (Hawkins et al. 2021; Liang et al. 2021; Zhang et al. 2021). Optical microscopy allowed the growth of the dissolved and coagulated fraction at various temperatures and times to be directly measured. The effect of addition of various concentrations of water on the dissolution speed and activation energy in cellulose/IL mixtures is studied with time-temperature superposition (TTS). These measurements displayed an Arrhenius behavior, which allowed the measurement of the required activation energy for the dissolution for each of water concentration to be determined. The effect of the addition of small amounts of water on dissolution speed is also investigated. The focus of this study is to understand and explore the fundamental science in order to ultimately prepare all-cellulose composites, where control of matrix fraction is needed for optimum mechanical properties. We believe that the results obtained in this study will be useful to future research on the production of all-cellulose composites (Chen et al. 2020b; Gindl and Keckes 2005; Nishino et al. 2004; Victoria et al. 2022). Flax fiber based composites provide a promising way of replacing manufacturing materials without significant environmental damage due to excellent mechanical performance, being fully bio-based and potential recyclability (Moudood et al. 2020).

Experimental material

Materials

Flax fibers were obtained from Airedale Yarns, Keighley, UK. Flax fibers were chosen to be the cellulose source which is formed from a continuous yarn fiber with a diameter of 0.5 mm. The solvent used was 1-ethyl-3-methyl-imidazolium acetate [C2mim] [OAc] with a purity $\geq 98\%$ which was purchased from Proionic GmbH, Grambach, Austria. Epoxy (Epoxicure, Cold Cure Mounting Resin from Buehler, UK) was used to embed samples to examine and measure the fraction of dissolved fibers at each set of processing conditions.

Preparation sample

Flax fiber threads were wound separately around a polytetrafluoroethylene (PTFE) Teflon picture frame of dimensions 5 cm × 5 cm, fixing both ends of each fiber bundle (Fig. 1a). Four separate fiber samples were wound onto each frame for testing, to give repeat measurements at the various chosen times and temperatures during processing (Fig. 1b). The IL [C2mim] [OAc] was used and first pre-heated in a PTFE tray for 1 h to stabilise at the chosen target temperature before the dissolution experiments were commenced. Then, the frames were submerged into the Teflon dishes which were filled with the IL [C2mim] [OAc] (Fig. 1c), and then quickly returned to the vacuum oven (Fig. 1d). Shellab 17 L Digital Vacuum Oven SQ-15VAC-16, Sheldon Manufacturing, Inc.,
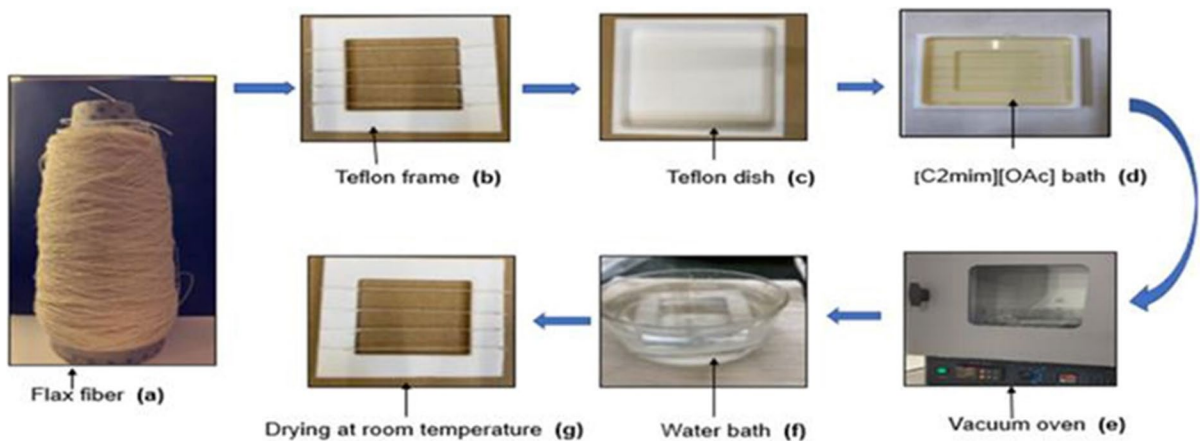
Fig. 1 The process of dissolving flax fiber bundles in [C2mim][Ac]

USA, was used to dissolve the flax samples at various temperatures and times (Fig. 1e). After the dissolving process, the flax fiber samples were removed from the IL [C2mim] [OAc] and then immediately soaked in a water bath for 24 h at room temperature to coagulate the dissolved cellulose, as shown in (Fig. 1f), and the used IL [C2mim] [OAc] was collected for recycling. A drying process was employed after removing the fibers from the water bath, leaving to dry for more than 24 h at room temperature before cutting the samples from the frame (Fig. 1g).

Characterization and qualification

Optical microscopy

Optical microscopy (BH2-Olymous Corporation, Japan) was used in conjunction with a CCD (Charge-coupled- device) camera to analyse the cross- sectional images of the microstructures of both the flax fibre bundles (raw fibres) and the partially dissolved (composite fibres). Epoxy resin was used to encapsulate the fiber samples for optical microscopy. Each set of four samples were embedded in an epoxy resin, which were then ground down and polished to the fiber surface before examining in reflection to allow for clear images, as shown in Fig. 2. To measure the ratio between the raw fibers (undissolved fiber, inner area) and the coagulated fraction (dissolved fiber, outer area), ImageJ processing software was used, as shown in Fig. 3. The coagulated fraction CF was calculated using,

$$CF = A_C/A_T \qquad (1)$$

where A_C is the area of the cross-sectional of the coagulated cellulose and A_T is the total area of cross- sectional for coagulated cellulose plus raw cellulose.

Fig. 2 The epoxy resin embedding method. **a** Flax fiber bundles were embedded in an epoxy resin, **b** fiber threads before grounding down and polishing, **c** fibers after fully curing to allow clear images
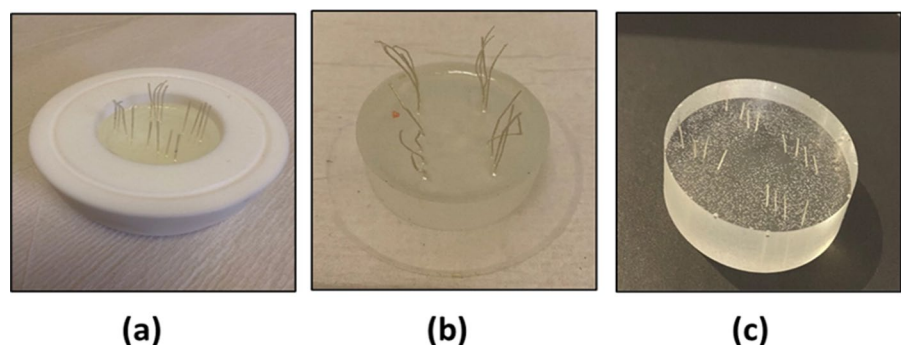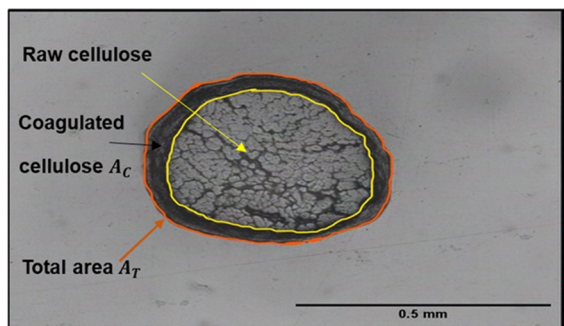
Fig. 3 A partially dissolved fiber shows the raw cellulose (inner core), the coagulated cellulose area and the total area of both raw and coagulated fiber (outer layer)

Antisolvent distilled water

The antisolvent (distilled water) was mixed into the IL with a magnetic stirrer for 10 min prior to use. Three water concentrations were used: 1%, 2% and 4% by weight. We have chosen 4 wt% water as our upper limit, for when we exceed this, the dissolution process became too slow to be practically observed. This result is in line with a publication that demonstrated only swelling of single flax fibers occurred in this IL, when containing 5 wt% water (Chen et al. 2020a).

Karl Fisher Titration (KFT) was used before and after the dissolution process to determine the amount of water content of the IL. KFT on the IL as received from the manufactures Proionic, showed this to contain 0.2% water. By adding 0.8% water to the original 0.2% water to make 1%, 1.8% water added to make 2% water, and 3.8% water added to make 4% water. The IL/water mixture exhibits a much higher vapor pressure and may thus evaporate under vacuum. Thus, the vacuum oven atmosphere was replaced with a nitrogen atmosphere to avoid evaporation. Several researchers have studied the interaction between [C2mim] [OAc] and water and found that their properties could be significantly changed in the presence of water; for example, the melting point, polarity, viscosity and surface tension of ILs are changed (Duchemin et al. 2014; Jacquemin et al. 2006; Reid et al. 2017; Zhou et al. 2020).

## Results and discussion

Optical data

Figure 4 is a representation of typical micrographs of both raw fibers and partially dissolved fibers that were processed at various times at 50 °C. These are very similar to a previous study in this group investigating the dissolution of flax fibers in the IL [C2mim][OAc] as manufactured by Sigma Aldrich (Hawkins et al. 2021). As shown, a raw fiber bundle is made up of various bundles which are tightly packed together with minimal internal free space. This appears to prevent the ionic liquid from penetrating the core, and so the dissolution proceeds from the outer edges inwards. The micrographs suggest that we can consider the partially dissolved composite fibers to be comprised of an inner undissolved core surrounded by a ring of dissolved and coagulated cellulose. A number of typical images representing raw fibers can be seen in SI Fig. 1.

The processed fibers, seen in Fig. 4a-d, processed at 50 °C, shows how the inner undissolved area is surrounded by an outer layer whose size depends on the processing time and that this increases as time increases. These outer layers are the result of cellulose that was through the dissolution and coagulation process.

To measure the boundaries between the inner core and partially dissolved area, as well as the partially dissolved area and the outer area, a Software (Image J) was used to trace out each boundary by eye and the ratios between inner and outer boundaries were averaged across four repeat samples made at each set of processing conditions, the area enclosed within these boundaries is used to determine the coagulated fraction and the raw material, as seen in Fig. 4. The coagulation fraction (CF) is calculated by Eq. 1 given above.

In Fig. 5 is shown the results of the growth of the coagulation fraction of the fibers processed at different temperatures and times. On this figure, the data represents the average value of the coagulation fraction taken from the four cross-sectional fibers processed under the same time and temperature, and the error bar is the standard error. Therefore, the CF is seen to increase as a function of both processing time and the processing temperature.
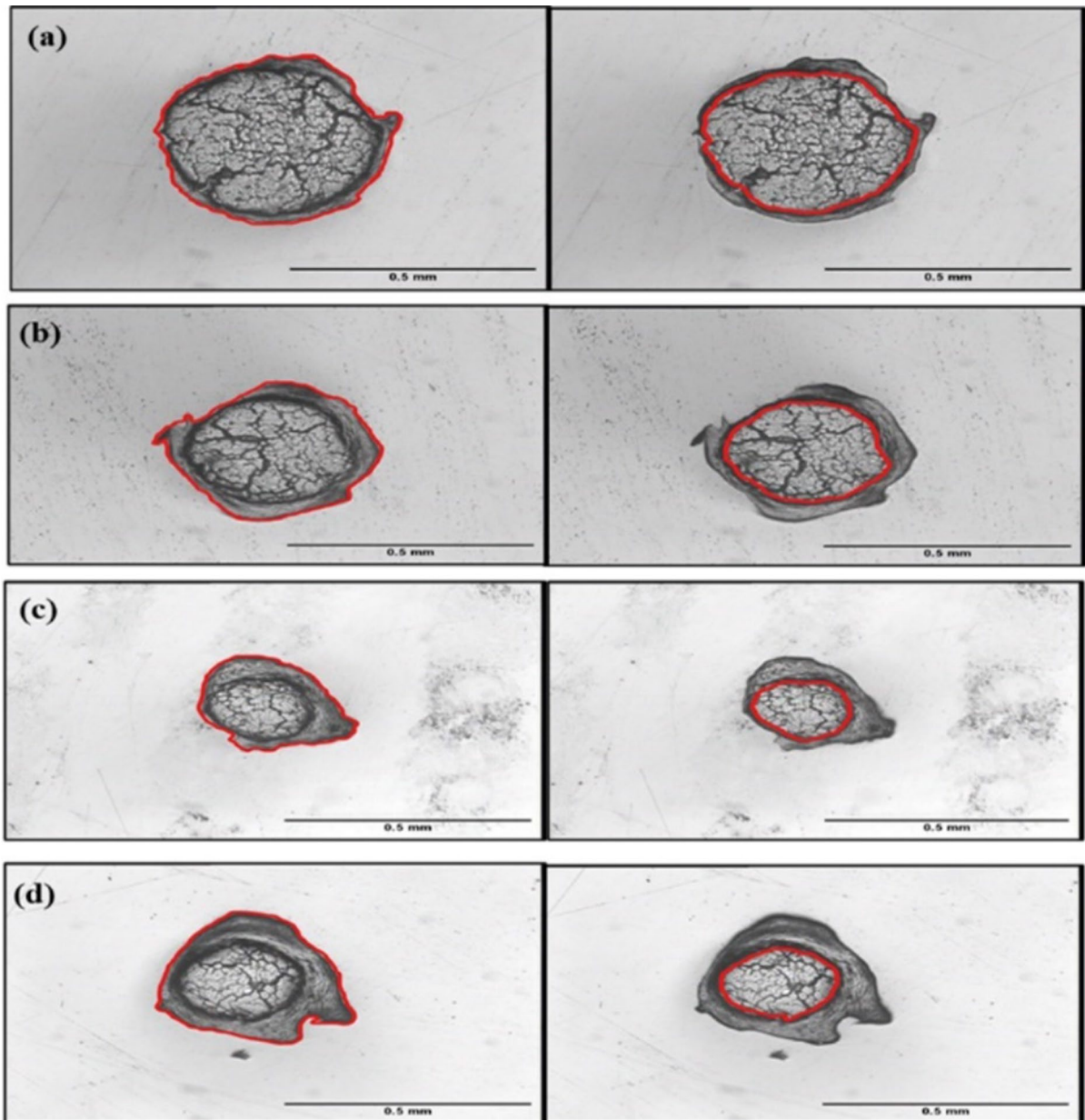
Fig. 4 Microscopy images showing how the boundaries between raw and partially dissolved cellulose were determined. The outer boundary is shown on the left and the inner on the right. Fibers shown were dissolved at 50 °C for **a** 0.5 h, **b** 1 h, **c** 1.5 h and **d** 2 h. Scale length 0.5 mm

In Fig. 5 it can be seen that the CF grows with time at each processing temperature and grows faster as the processing temperature is increased. The data in Fig. 6a illustrates how each individual curve in Fig. 5 could be collated to show the relation between the dissolution time and temperature by applying the concept of time temperature superposition, in order to create a master curve at each specific temperature. The process used to form a master curve is to shift different temperature curves horizontally along the logarithmic time (ln time) axis in order to achieve the best overlap via Eqs. 2 and 3.

Fig. 5 Coagulated fraction as a function of dissolution time at different temperatures. Polynomial function used in order to guide the eye and error bars included
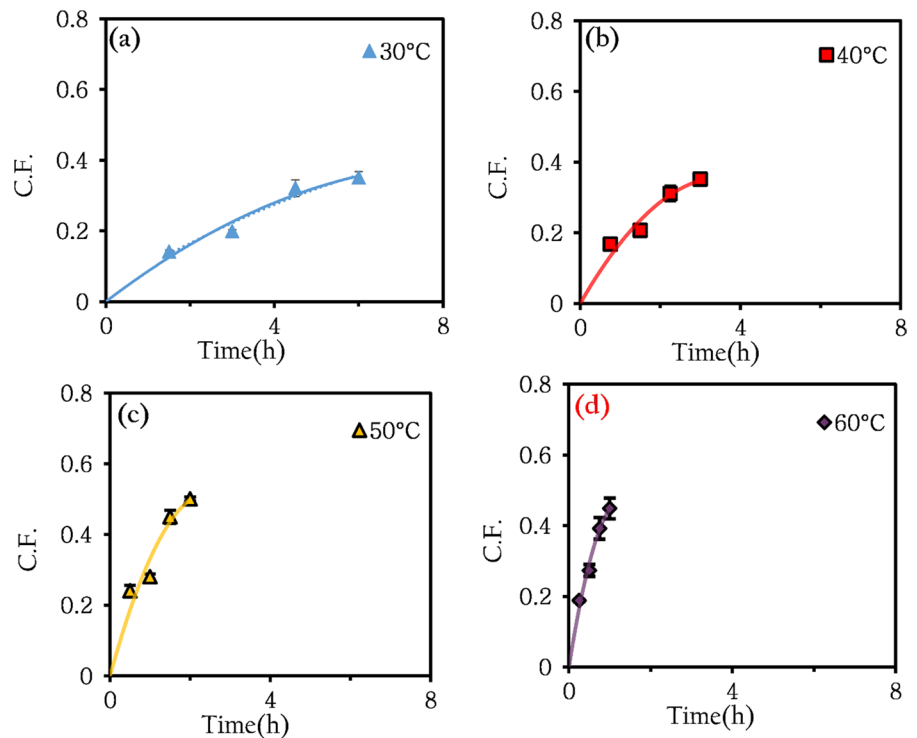
$$t' = t \times \alpha_T \tag{2}$$

By taking the natural log of both sides of the Eq. 2 yields the following:

$$\ln(t') = \ln(t) \times \ln(\alpha_T) \tag{3}$$

where t′ is the shifted dissolution time, t is the dissolution time and $\ln(\alpha_T)$ is the shift factor to move the data from temperature T to the reference temperature T_{ref}

Figure 6b shows schematically the creation of the master curve, which contained a number of steps to construct the best master curve by using the middle temperature, $T_{ref} = 50$ °C, as the reference set with therefore scaling factor $\alpha_{50} = 1$. The 50 °C data was fitted with a preliminary polynomial function used to guide the eye in order to provide the best shifting of further data sets, see Fig. 6c. Then, each of the other data curves 30 °C, 40 and 60 °C was horizontally shifted separately along the x- axis (ln time) by a shift factor equal to $\ln(\alpha_T)$ towards the reference temperature to make them overlap, see Fig. 6. This procedure is similar to that performed in rheological analysis, when studying

time- temperature-superposition (TTS). After shifting of the data sets, the master curve is formed (at 50 °C), as shown in Fig. 6d. This polynomial master curve shows superimposed data set with $R^2 \gtrsim 0.99$. Finally, the R^2 value was maximized via adjusting the shift factors at the other temperatures (α_{30}, α_{40} and α_{60}) to provide the best fit between the shifted points and the polynomial fitted. Optical microscopy cross sections also documenting the proposed interchangeability of time and temperature can be found in SI Fig. 2.

We can now plot the four shift factors $\ln(\alpha_T)$ for the data against the inverse of temperature (T^{-1}), as shown in Fig. 6e. The linear nature of these data indicates that the dissolution process follows Arrhenius behaviour. The equation below representing the activation energy (E_a) describes the energy barrier required for the dissolution of flax fibers in [C2mim] [OAc] that needs to be overcome for dissolution to occur. The dissolution activation energy of the flax fiber in [C2mim] [OAc] was calculated, using the slope shown in Fig. 6e, to be 64 ± 5 kJ/mol. The uncertainty comes from the uncertainty from the linear regression fitting and is found using (LINEST in EXCEL)

Fig. 6 **a** CF as a function of both dissolution time and temperature. **b** CF at various times and temperatures expressed in ln(*time*). **c** The shifting process, by moving the 30 °C ,40 and 60 °C data towards the 50 °C data. **d** The final master curve shows the effect of dissolution time and temperature on the coagulation fraction. **e** The linear nature of the data showing shift factors ln(α_T) as a function of temperature, an Arrhenius plot
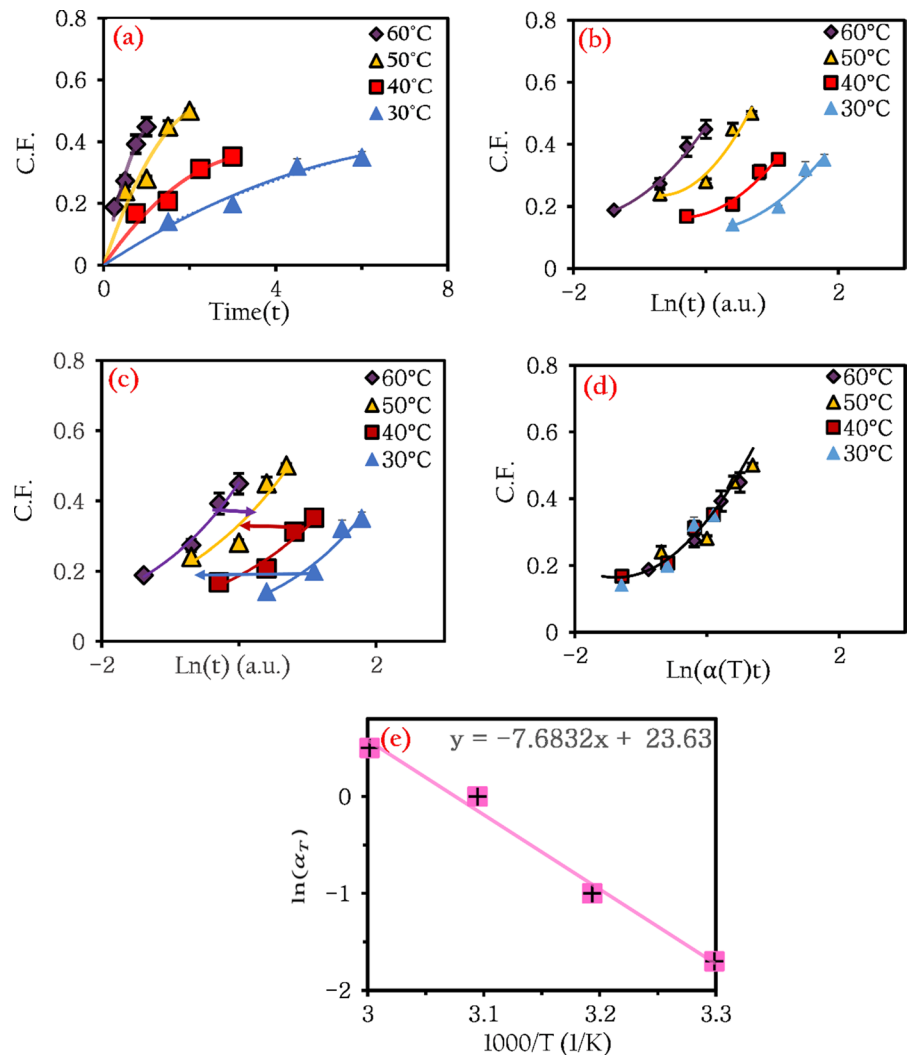
$$\alpha_T = \alpha_0 e^{\frac{-E_a}{RT}} \tag{4}$$

$$\ln\left(\alpha_T\right) = \left(\frac{-E_a}{RT}\right) + \ln\alpha_0 \tag{5}$$

where α_T is the scaling factor, E_a is the Arrhenius activation energy, R is the gas constant, T is the temperature in kelvin and is α_0 the pre-exponential factor.

Intercept method (lnα_0)

This method uses the other parameter from the Arrhenius plots of the shift factors versus inverse temperature, namely the intercept ln α_0 from Eq. 5. The process used to obtain the intercept from the Arrhenius

plot curve was described in detail for a reference temperature of 50 °C. Figure 6e showed that this gave a gradient of −7.6832x and an intercept of 23.63.

If all of the above analysis is carried out again three times, now using the other three temperatures as reference temperatures (T_{ref}), so shifting all data to 30 and 40 °C and finally 60 °C in order to create a master curve for each set of data at each of these temperatures. The shift factors, from 30 °C, 40 and 60 °C TTS shifting, can be plotted separately as a function of temperature as before for the 50 °C TTS shifting results. Each set of shift factors for each of the reference temperatures is again found to display an Arrhenius behaviour, each giving a dissolution activation energy, see Fig. 7a-c. These plotted graphs give similar gradients, leading to similar E_a as calculated from 50 °C (64±5

Fig. 7 Shift factors $\ln\left(\alpha_{T_{ref}}\right)$ as a function of inverse temperature, indicating Arrhenius plot. Reference temperatures of **a** 30 °C, **b** 40 °C, **c** 60 °C and **d** Intercept process, showing shifting to all temperatures indicating Arrhenius dependence
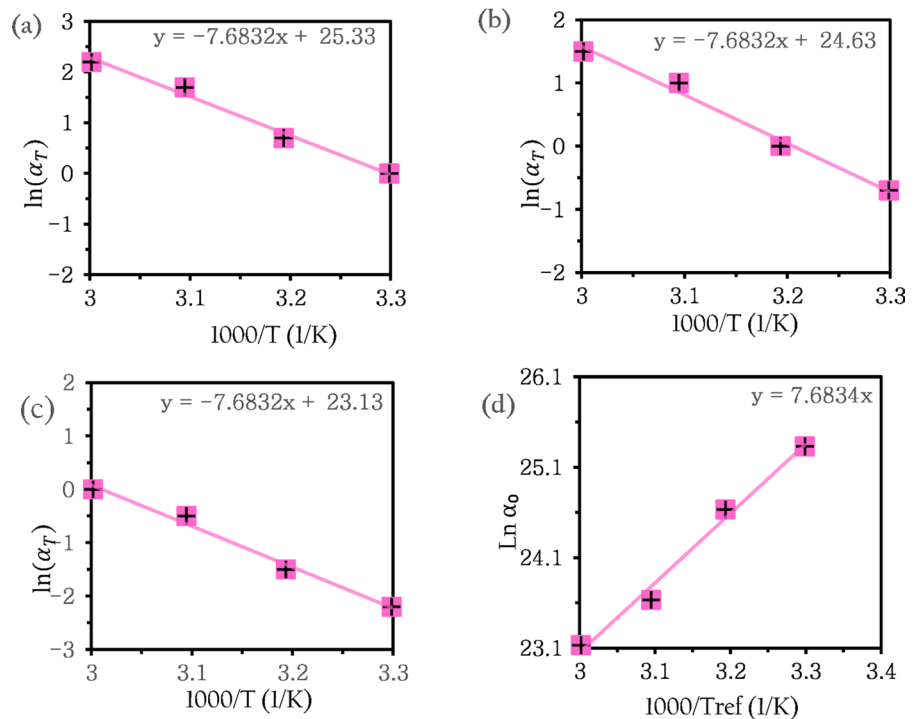
kJ/mol). The important result is that intercept $\ln\alpha_0$ in each of these graphs is itself temperature dependent $\ln\alpha_{30}$, $\ln\alpha_{40}$, and $\ln\alpha_{60}$. The intercepts are 25.33, 24.63, and 23.13 for 30 °C Fig. 7a, 40 °C Fig. 7b, and 60 °C Fig. 7c, respectively. These intercepts can then be checked to further verify the Arrhenius behaviour, as follows.

Firstly, we set the temperature T as the reference temperature T_{ref}, in Arrhenius Eq. 5, this then gives,

$$\ln\left(\alpha_{T_{ref}}\right) = \left(\frac{-E_a}{RT_{ref}}\right) + \ln\alpha_0 \qquad (6)$$

The shift factor at the reference temperature has to equal zero $\ln\left(\alpha_{T_{ref}}\right) = 0$, since the reference temperature data itself needs no shifting $\alpha_{T_{ref}} = 1$. Next, by substituting the value of $\ln\left(\alpha_{T_{ref}}\right) = 0$ in Eq. 6, rearranging Eq. 7 to be Eq. 8,

$$0 = \left(\frac{-E_a}{RT_{ref}}\right) + \ln\alpha_0 \qquad (7)$$

$$\ln\alpha_0 = \left(\frac{E_a}{RT_{ref}}\right) \qquad (8)$$

This expression above shows that the intercepts $\ln\alpha_0$ determined at each reference temperature themselves will follow an Arrhenius law, being linearly dependent on the inverse of the reference temperature. The gradient of the $\ln\alpha_0$ versus $1000/T_{ref}$ is predicted to give the activation energy, and this is a further confirmation that the system is exhibiting Arrhenius behavior, see Fig. 7d. In our work we have found that this analysis is very sensitive to any curvature or non-Arrhenius behaviour.

This 'intercept' method was applied as another method to measure the activation energy and compared with the activation energy for each master curve. The gradient of the line in Fig. 7d shows a very similar gradient as the Arrhenius plots in Fig. 6e and 7a-c, and hence gave a fifth value for the activation energy of 64 ± 5 kJ/mol, consistent with our previous determined values.

A number of other studies have shown the dissolution process has an Arrhenius behaviour. A cotton dissolution activation energies of 96 ± 8 kJ/mol and in [C2mim] [OAc] reported by Liang et al. (Liang et al. 2021). Zhang et al. (2021) reported that the activation energy needed to dissolve silk via a solvent [C2mim] [OAc] is 138 ± 13 kJ/mol(Zhang et al. 2021) The dissolution rate of cellulose fibers was found to be

Fig. 8 Master curves of coagulation fraction CF as function of ln(α_T) for each water system at 50 °C **a** 1%, **b** 2% and **c** 4% anti-solvent. The required activation energies of dissolution flax fiber in [C2mim] [OAc] as a function of water concentration a polynomial fit is used to guide the eye within their error bars (**d**)
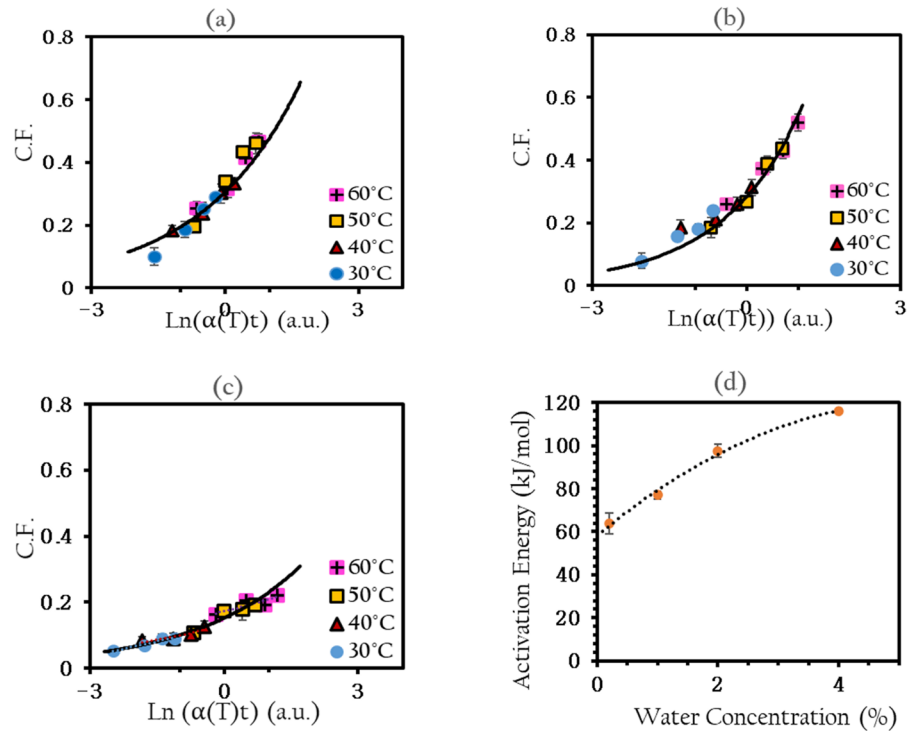
linearly related with the viscosity of [C2mim] [OAc] when both are expressed in natural logarithmic form. Furthermore, the dissolution shows Arrhenius behaviour (Chen et al. 2020a). The activation energies have shown to be dependent on the IL used and the concentration of cellulose, documented from 46 kJ/mol to approximately 70 kJ/mol in these different studies. Villar et al. (2023) reported that the activation energy needed to dissolve lyocell yarn via a solvent [C2mim] [OAc] is 46.8 kJ/mol, this result was reduced by 70% when DMSO was added (Villar et al. 2023).

**The effect of water on the activation energy and dissolution speed**

The mechanism of the dissolution observed in the IL with the water anti-solvent system was found to be similar as that of the pure IL system; with the inner fiber area surrounded by various outer layers, with the formation of the coagulation fraction around the core. The main difference seen when using water is the coagulation fraction decreases in size as a function of water content (at a fixed temperature and time). The rate at which fibers dissolve at various concentrations fell significantly, indicating that water is acting

to decrease the dissolution rate. Optical microscopy cross sections documenting the decreasing coagulated fraction as function of water concentration can be found in SI Fig. 3.

The antisolvent master curves generated for the 1%, 2% and 4% water systems separately following the same procedure as shown before in Fig. 6. First, the data at 50 °C was chosen to be the reference set with a scaling factor $\alpha_{50} = 1$. Then, all of the previous analysis was applied to these data sets, the result of which can be seen in Fig. 8a–c. The data represents the average value of the coagulation fraction taken from the four cross-sectional fibers processed under the same condition of time and temperature, and the error bar is the standard error. These three systems all likewise obeyed Arrhenius behaviour when using water as an antisolvent.

For 1%, 2% and 4% water systems, the activation energies were found to be 77 ± 2 kJ/mol, 97 ± 3 kJ/mol and 116 ± 0.6 kJ/mol respectively. Figure 8d displays the activation energy increase as a function of water concentration. An extrapolation was used for the theoretical dry IL 0% water to be 58 ± 4 kJ/mol. A polynomial function of order two was used to fit the data and extrapolate to zero water concentration.

Fig. 9 a Master curve representing all the results for the coagulation fraction as function of antisolvent concentration. **b** Relative dissolution rate of flax fibers as a function of antisolvent concentration. Exponential curve is a fit to the data
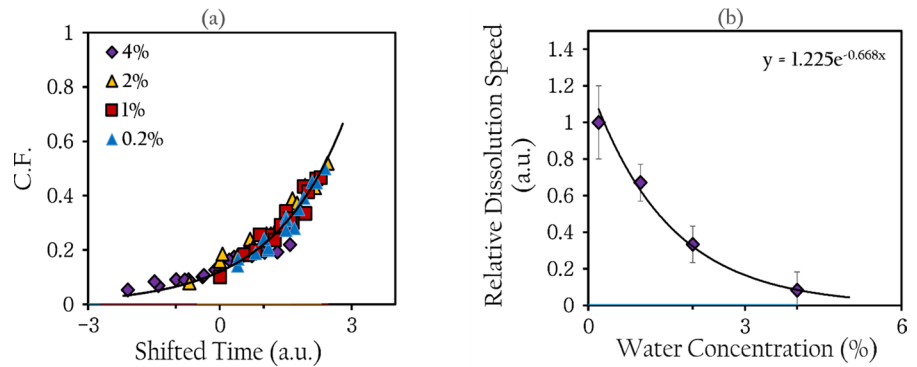
To calculate the relative dissolution rate between water systems, the procedure above repeated again for the 1%, 2% and 4% water systems with now each master curve itself shifted separately in natural logarithmic time to overlap with the master curve of 0.2% water results, shown before in Fig. 6(d), in order to measure the relative dissolution rate between the 1%, 2% and 4% water systems to that of the 0.2% water content of the IL as received from the manufacturer. So for example, to overlap the 2% water solvent with the master curve of 0.2% water solvent, needed a scaling factor α of 0.33, determined from the shift factor $\ln(\alpha)$. Hence, the dissolution rate is 3.3 times slower at this concentration $\left(\frac{1}{\alpha}\right)$. The resulting master curve including all water systems is seen in Fig. 9a. Figure 9b shows that the relative dissolution rate decreased exponentially as a function of water concentration, where we set the rate for the 'as received' IL equal to 1 (0.2% water).

The decreasing rate of dissolution is thought to be related to the water molecules crowding the anion h-bond sites, which prevented the interactions between the IL and the cellulose (Rabideau and Ismail 2015). Within their simulations, they discussed the interaction between cellulose, water and several ILs. They demonstrated that anions have the ability to form up to four hydrogen bonds with cellulose. By adding water, there was a strong disturbance in the frequency of hydrogen bonds between the anion and cellulose. This disturbance occurred because the water molecules occupied the hydrogen-bond accepting positions of the anion, preventing it from interacting with cellulose. It was demonstrated that as the amount of water increased, the crowding of these positions becomes more prominent. The

authors suggest that the presence of water leads to a significant reduction in hydrogen bonding between anions and cellulose, and this may account for the rapid decline observed in the dissolution rate. This also agrees with experimental work done by Koide et al. which reported that the interaction between water molecules and [C2mim][Ac] is stronger than the [C2mim][Ac] with cellulose (Koide et al. 2020).

From the exponential function in Fig. 9b, the following equation obtained:

$$Y = 1.225e^{-0.668x} \tag{9}$$

where Y is the relative dissolution speed (relative to the IL as purchased) and x is the water concentration in weight%.

This equation suggests that flax fibers would dissolve 23% faster at 0% water content, in a theoretically perfectly dry IL. For every 1% of additional water the rate decreases by 49%, or in otherwards the dissolution takes twice as long.

Conclusion

The dissolution of flax fibers in the ionic liquid [C2mim] [OAc] is studied with the addition of an anti-solvent, water as a function of dissolution times, temperatures and water anti-solvent concentration. The dissolution process allowed the partially dissolved flax composite fibers to be created, after which OM was used to analysis the morphology of dissolved fibers, and it was found that the core fiber is surrounded by a coagulated flax matrix phase as dissolution proceeded. The coagulation fraction became larger as a function of time and

temperature which was found to follow (TTS). The shift factors used to obtain the master curve across their dissolution temperatures show an Arrhenius behaviour in this system. As a result, an activation energy was measured to be 64 ± 5 kJ/mol. An "intercept method" was introduced, which is highly sensitive to any curvature in an Arrhenius type plot and confirmed the Arrhenius behaviour of our data. This method confirmed the activation energy 64 ± 5 kJ/mol.

The antisolvent water was found to decrease the rate of dissolution of flax fibers, accompanied by increase in the activation energy. For 1%, 2% and 4% water systems, the activation energies were found to be 77 ± 2 kJ/mol, 97 ± 3 kJ/mol and 116 ± 0.6 kJ/mol respectively. The relative dissolution rate of flax fibers as a function of antisolvent concentration decreased exponentially, for every 1% addition of water by weight the rate of dissolution is approximately halved. Extrapolating our results to zero water concentration gave a value for the pure IL (no water) dissolution activation energy of 58 ± 4 kJ/mol. Finally, the hypothetical dry ionic liquid (0% water) is predicted to dissolve cellulose 23% faster than the IL as received (0.2% water).

Data availability The datasets generated during and/or analysed in the current study are available from the corresponding author on request. The data associated with this paper are openly available from the University of Leeds Data Repository, https://doi.org/10.5518/1278.

Declarations

Conflict of interest The authors declare that they have no conflict of interest.

Consent to participate All authors consent to participating in this work.

Consent for publication All authors have given consent for this publication, which includes text, photographs, Figures and details within the text to be published in the journal "Cellulose".

References

Baranwal J, Barse B, Fais A, Delogu GL, Kumar A (2022) Biopolymer: a sustainable material for food and medical applications. Polymers 14(5):983. https://doi.org/10.3390/polym14050983

Bochek A (2003) Effect of hydrogen bonding on cellulose solubility in aqueous and nonaqueous solvents. Russ J Appl Chem 76(11):1711–1719. https://doi.org/10.1023/B:RJAC.0000018669.88546.56

Brehm M, Pulst M, Kressler J, Sebastiani D (2019) Triazolium-based ionic liquids: a novel class of cellulose solvents. J Phys Chem B 123(18):3994–4003. https://doi.org/10.1021/acs.jpcb.8b12082

Chen F, Sawada D, Hummel M, Sixta H, Budtova T (2020) Swelling and dissolution kinetics of natural and man-made cellulose fibers in solvent power tuned ionic liquid. Cellulose 27(13):7399–7415. https://doi.org/10.1007/s10570-020-03312-5

Chen F, Sawada D, Hummel M, Sixta H, Budtova T (2020) Unidirectional all-cellulose composites from flax via controlled impregnation with ionic liquid. Polymers 12(5):1010. https://doi.org/10.3390/polym12051010

Duchemin BJ, Staiger MP, Newman RH (2014) High-Temperature Viscoelastic Relaxation in All-Cellulose Composites Paper presented at the Macromolecular Symposia

Earle MJ, Esperança JM, Gilea MA, Lopes JNC, Rebelo LP, Magee JW, Seddon KR, Widegren JA (2006) The distillation and volatility of ionic liquids. Nature 439(7078):831–834. https://doi.org/10.1038/nature04451

Fukaya Y, Hayashi K, Wada M, Ohno H (2008) Cellulose dissolution with polar ionic liquids under mild conditions: required factors for anions. Green Chem 10(1):44–46. https://doi.org/10.1039/B713289A

Fukaya Y, Sugimoto A, Ohno H (2006) Superior solubility of polysaccharides in low viscosity, polar, and halogen-free

1, 3-dialkylimidazolium formates. Biomacromolecules 7(12):3295–3297. https://doi.org/10.1021/bm060327d

Ghandi K (2014) A review of ionic liquids, their limits and applications. Green Sustain Chem. http://www.scirp.org/journal/PaperInformation.aspx?PaperID=43349

Gindl W, Keckes J (2005) All-cellulose nanocomposite. Polymer 46(23):10221–10225. https://doi.org/10.1016/j.polymer.2005.08.040

Gupta KM, Hu Z, Jiang J (2013) Cellulose regeneration from a cellulose/ionic liquid mixture: the role of anti-solvents. RSC Adv 3(31):12794–12801. https://doi.org/10.1039/C3RA40807H

Hall CA, Le KA, Rudaz C, Radhi A, Lovell CS, Damion RA, Budtova T, Ries ME (2012) Macroscopic and microscopic study of 1-ethyl-3-methyl-imidazolium acetate–water mixtures. J Phys Chem B 116(42):12810–12818. https://doi.org/10.1021/jp306829c

Hawkins JE, Liang Y, Ries ME, Hine PJ (2021) Time temperature superposition of the dissolution of cellulose fibres by the ionic liquid 1-ethyl-3-methylimidazolium acetate with cosolvent dimethyl sulfoxide. Carbohydr Polym Technol Appl 2:100021. https://doi.org/10.1016/j.carpta.2020.100021

Huber T, Müssig J, Curnow O, Pang S, Bickerton S, Staiger MP (2012) A critical review of all-cellulose composites. J Mater Sci 47(3):1171–1186. https://doi.org/10.1007/s10853-011-5774-3

Jacquemin J, Husson P, Padua AA, Majer V (2006) Density and viscosity of several pure and water-saturated ionic liquids. Green Chem 8(2):172–180. https://doi.org/10.1039/B513231B

Ju Z, Yu Y, Feng S, Lei T, Zheng M, Ding L, Yu M (2022) Theoretical mechanism on the cellulose regeneration from a cellulose/EmimOAc mixture in anti-solvents. Materials 15(3):1158. https://doi.org/10.3390/ma15031158

Khademian E, Salehi E, Sanaeepur H, Galiano F, Figoli A (2020) A systematic review on carbohydrate biopolymers for adsorptive remediation of copper ions from aqueous environments-part A: classification and modification strategies. Sci Total Environ 738:139829. https://doi.org/10.1016/j.scitotenv.2020.139829

Khan AS, Man Z, Bustam MA, Kait CF, Nasrullah A, Ullah Z, Sarwono A, Ahamd P, Muhammad N (2018) Dicationic ionic liquids as sustainable approach for direct conversion of cellulose to levulinic acid. J Clean Prod 170:591–600. https://doi.org/10.1016/j.jclepro.2017.09.103

Koide M, Urakawa H, Kajiwara K, Rosenau T, Wataoka I (2020) Influence of water on the intrinsic characteristics of cellulose dissolved in an ionic liquid. Cellulose 27:7389–7398. https://doi.org/10.1007/s10570-020-03323-2

Le KA, Sescousse R, Budtova T (2012) Influence of water on cellulose-EMIMAc solution properties: a viscometric study. Cellulose 19(1):45–54. https://doi.org/10.1007/s10570-011-9610-3

Li X, Li H, Ling Z, Xu D, You T, Wu Y-Y, Xu F (2020) Room-temperature superbase-derived ionic liquids with facile synthesis and low viscosity: powerful solvents for cellulose dissolution by destroying the cellulose aggregate structure. Macromolecules 53(9):3284–3295. https://doi.org/10.1021/acs.macromol.0c00592

Li Y, Wang J, Liu X, Zhang S (2018) Towards a molecular understanding of cellulose dissolution in ionic liquids: anion/cation effect, synergistic mechanism and physico-chemical aspects. Chem Sci 9(17):4027–4043. https://doi.org/10.1039/C7SC05392D

Liang Y, Hawkins JE, Ries ME, Hine PJ (2021) Dissolution of cotton by 1-ethyl-3-methylimidazolium acetate studied with time–temperature superposition for three different fibre arrangements. Cellulose 28(2):715–727. https://doi.org/10.1007/s10570-020-03576-x

Liebner F, Patel I, Ebner G, Becker E, Horix M, Potthast A, Rosenau T (2010) Thermal aging of 1-alkyl-3-methylimidazolium ionic liquids and its effect on dissolved cellulose. Walter de Gruyter, Berlin. https://doi.org/10.1515/hf.2010.033

Lindman B, Medronho B, Alves L, Costa C, Edlund H, Norgren M (2017) The relevance of structural features of cellulose and its interactions to dissolution, regeneration, gelation and plasticization phenomena. Phys Chem Chem Phys 19(35):23704–23718. https://doi.org/10.1039/C7CP02409F

Liu N, Li Z, Chen S, Wang H (2015a) Novel fibres prepared by cellulose diacetate using ionic liquid as plasticiser. Mater Res Innov 19(sup9):S9-295-S299-298. https://doi.org/10.1179/1432891715Z.0000000001991

Liu X, Zhou G, He H, Zhang X, Wang J, Zhang S (2015) Rod-like micelle structure and formation of ionic liquid in aqueous solution by molecular simulation. Ind Eng Chem Res 54(5):1681–1688. https://doi.org/10.1021/ie503109z

Manna B, Ghosh A (2019) Dissolution of cellulose in ionic liquid and water mixtures as revealed by molecular dynamics simulations. J Biomol Struct Dyn 37(15):3987–4005. https://doi.org/10.1080/07391102.2018.1533496

Mazlan NSN, Zakaria S, Gan S, Hua CC, Baharin KW (2019) Comparison of regenerated cellulose membrane coagulated in sulphate based coagulant. Cerne 25:18–24. https://doi.org/10.1590/01047760201925012586

Mazza M, Catana D-A, Vaca-Garcia C, Cecutti C (2009) Influence of water on the dissolution of cellulose in selected ionic liquids. Cellulose 16(2):207–215. https://doi.org/10.1007/s10570-008-9257-x

Miao C, Hamad WY (2013) Cellulose reinforced polymer composites and nanocomposites: a critical review. Cellulose 20(5):2221–2262. https://doi.org/10.1007/s10570-013-0007-3

Miyamoto H, Schnupf U, Brady JW (2014) Water structuring over the hydrophobic surface of cellulose. J Agric Food Chem 62(46):11017–11023. https://doi.org/10.1021/jf501763r

Moudood A, Rahman A, Huq NML, Öchsner A, Islam MM, Francucci G (2020) Mechanical properties of flax fiber-reinforced composites at different relative humidities: experimental, geometric, and displacement potential function approaches. Polym Compos 41(12):4963–4973. https://doi.org/10.1002/pc.25766

Nishino T, Matsuda I, Hirao K (2004) All-cellulose composite. Macromolecules 37(20):7683–7687. https://doi.org/10.1021/ma049300h

Plechkova NV, Seddon KR (2008) Applications of ionic liquids in the chemical industry. Chem Soc Rev 37(1):123–150. https://doi.org/10.1039/B006677J

Rabideau BD, Ismail AE (2015) Mechanisms of hydrogen bond formation between ionic liquids and cellulose and the influence of water content. Phys Chem Chem Phys 17(8):5767–5775. https://doi.org/10.1039/C4CP04060K

Reid JE, Gammons RJ, Slattery JM, Walker AJ, Shimizu S (2017) Interactions in water–ionic liquid mixtures: comparing protic and aprotic systems. J Phys Chem B 121(3):599–609. https://doi.org/10.1021/acs.jpcb.6b10562

Rosenau T, Potthast A, Kosma P, Chen C-L, Gratzl JS (1999) Autocatalytic decomposition of *N*-methylmorpholine *N*-oxide induced by Mannich intermediates. J Org Chem 64(7):2166–2167

Swatloski RP, Spear SK, Holbrey JD, Rogers RD (2002) Dissolution of cellose with ionic liquids. J Am Chem Soc 124(18):4974–4975. https://doi.org/10.1021/ja025790m

Tan X, Chen L, Li X, Xie F (2019) Effect of anti-solvents on the characteristics of regenerated cellulose from 1-ethyl-3-methylimidazolium acetate ionic liquid. Int J Biol Macromol 124:314–320. https://doi.org/10.1016/j.ijbiomac.2018.11.138

Taokaew S, Kriangkrai W (2022) Recent progress in Processing cellulose using ionic liquids as solvents. Polysaccharides 3(4):671–691. https://doi.org/10.3390/polysaccharides3040039

Victoria A, Ries ME, Hine PJ (2022) Use of interleaved films to enhance the properties of all-cellulose composites. Compos Part A Appl Sci Manuf. https://doi.org/10.1016/j.compositesa.2022.107062

Villar L, Pita M, Paez J, Sánchez PB (2023) Dissolution kinetics of cellulose in ionic solvents by polarized light microscopy. Cellulose. https://doi.org/10.1007/s10570-022-05036-0

Walden P (1914) Molecular magnitude and electrical conductivity of some fused salts. Bull Acad Imp Sci St Petersb 6:405–422

Yang J, Lu X, Yao X, Li Y, Yang Y, Zhou Q, Zhang S (2019) Inhibiting degradation of cellulose dissolved in ionic liquids via amino acids. Green Chem 21(10):2777–2787. https://doi.org/10.1039/C9GC00334G

Yang G, Song Y, Wang Q, Zhang L, Deng L (2020) Review of ionic liquids containing, polymer/inorganic hybrid electrolytes for lithium metal batteries. Mater Des 190:108563. https://doi.org/10.1016/j.matdes.2020.108563

Yang X, Wang Q, Yu H (2014) Dissolution and regeneration of biopolymers in ionic liquids. Russ Chem Bull 63(3):555–559. https://doi.org/10.1007/s11172-014-0471-4

Zeng B, Wang X, Byrne N (2020) Cellulose beads derived from waste textiles for drug delivery. Polymers 12(7):1621. https://doi.org/10.3390/polym12071621

Zhang X, Ries ME, Hine PJ (2021) Time–temperature superposition of the dissolution of silk fibers in the ionic liquid 1-ethyl-3-methylimidazolium acetate. Biomacromolecules 22(3):1091–1101. https://doi.org/10.1021/acs.biomac.0c01467

Zhang H, Wu J, Zhang J, He J (2005) 1-Allyl-3-methylimidazolium chloride room temperature ionic liquid: a new and powerful nonderivatizing solvent for cellulose. Macromolecules 38(20):8272–8277. https://doi.org/10.1021/ma0505676

Zhao Y, Wang J, Wang H, Li Z, Liu X, Zhang S (2015) Is there any preferential interaction of ions of ionic liquids with DMSO and H_2O? A comparative study from MD simulation. J Phys Chem B 119(22):6686–6695. https://doi.org/10.1021/acs.jpcb.5b01925

Zhou G, Jiang K, Wang Z, Liu X (2020) Insight into the behavior at the hygroscopicity and interface of the hydrophobic imidazolium-based ionic liquids. Chin J Chem Eng. https://doi.org/10.1016/j.cjche.2020.09.047

Zweckmair T, Hettegger H, Abushammala H, Bacher M, Potthast A, Laborie M-P, Rosenau T (2015) On the mechanism of the unwanted acetylation of polysaccharides by 1,3-dialkylimidazolium acetate ionic liquids: part 1—analysis, acetylating agent, influence of water, and mechanistic considerations. Cellulose 22:3583–3596. https://doi.org/10.1007/s10570-015-0756-2